Inorg. Chem. 1991, 30, 294-299

Contribution from the Dipartimento di Chimica Inorganica, Chimica Fisica e Chimica dei Materiali, Università di Torino,
via P. Giuria 7, 10125 Torino, Italy, Eidgenössische Technische Hochschule, Universitätstrasse 6, CH-8092 Zürich, Switzerland,
and Dipartimento di Chimica, Università di Sassari, via Vienna 2, 07100 Sassari, Italy

$Co_6(\mu_3\text{-}S)_8(CO)_6\cdot 3S_8$. Structure, Bonding, and Vibrational Analysis of an Exceptionally Electron-Rich Carbonyl Cluster

E. Diana,[†] G. Gervasio,[†] R. Rossetti,[†] F. Valdemarin,[†] G. Bor,[‡] and P. L. Stanghellini*,[§]

Received February 14, 1990

The title complex is the main product of the room-temperature reaction between $Co_2(CO)_8$ and sulfur. Its crystals are monoclinic, space group $C2/c$, with $a = 20.456$ (4) Å, $b = 12.385$ (4) Å, $c = 17.600$ (5) Å, $\beta = 90.94$ (2)°, and $Z = 4$. The structure was solved by the heavy-atom method and refined by full-matrix least-squares techniques to the conventional $R(F_o)$ value of 0.048 for 3395 reflections having $F > 6\sigma(F)$. The structure of the cluster can be described as a Co_6 octahedron (mean Co–Co distance 2.81 Å) inserted in a S_8 cube (mean nonbonded S···S distance 3.09 Å). Each sulfur atom caps the triangular Co_3 faces, and one CO group is terminally bonded to each cobalt atom. The idealized symmetry is O_h. The S_8 rings are distant enough from the molecules of the cluster to exclude any chemical interaction between them. A qualitative description of the bonding (49 accessible MO's to accommodate the 98 valence electrons) is compared with that of the common octahedral metal clusters (43 MO's and 86 valence electrons). Detailed calculations on similar molecular complexes ($Cp_6M_6(\mu_3S)_8$) and solid-state structures ("Chevrel phases") give insights to a qualitative understanding of the chemical and structural properties of the cluster. The analysis of the FT-infrared and Raman spectra leads to an assignment of the main vibrational modes of the coordinated CO groups (C–O and Co–CO stretch and Co–C–O deformation) and of the Co_6S_8 core (Co–S and Co–Co stretch).

Introduction[1]

Dicobalt octacarbonyl is distinguished among the simple isoleptic metal carbonyls by its extremely high reactivity toward various reactants under mild conditions (room temperature, hydrocarbon solvents) to yield a wide variety of more stable $Co_x(CO)_yL_z$ derivatives.[2]

The reaction of dicobalt octacarbonyl with cyclooctasulfur in alkane solution was first described more than 25 years ago.[3-5] The study of the reaction of $Co_2(CO)_8$ with different types of organic and inorganic sulfur compounds was, at that time, an outgrowth of the practical interest for the application of homogeneous catalytic methods for sulfur containing unsaturated cracked petroleum products.[6,7]

The studies with elemental sulfur resulted in the observation of four hexane-soluble compounds of the family $Co_x(CO)_yS_z$; three of them could be subsequently also structurally characterized as $Co_3(\mu_3\text{-}S)(CO)_9$ (I),[8] $[Co_3(\mu_3\text{-}S)(CO)_7]_2(\mu_4\text{-}S_2)$ (II),[9] and $Co_4(\mu_4\text{-}S)_2(CO)_{10}$ (III),[10] respectively. Compound I was identified also in the reaction product mixtures obtained with several mercaptans and disulfides, and also with CS_2.[11-14] The formula and the structure of the fourth soluble compound (IV) (labeled as "S-4" in ref 5), however, remained unresolved for a long time. The reason for this lack of success was a combination of several factors. On one hand, the compound showed an extremely high sulfur content (ca. 66%) as compared with the low cobalt content (23%), indicating a S/Co ratio of 5 or higher, and at the same time, on the other hand, it had only a single sharp C–O stretching band in the solution IR spectrum,[15] suggesting a very high symmetry. Therefore, it was difficult to propose a structural type to accommodate this high number of sulfur atoms within a highly symmetric molecule.

More recently by an improved synthetic route, we succeeded in preparing complex IV suitable for crystallographic characterization. This study revealed an unprecedented type of a hexacobalt octasulfide cluster, coexisting in the lattice with S_8 rings, the cluster/ring ratio being 1:3. The details are presented in this paper.

Experimental Section

Synthesis of Complex IV. A 0.480-g sample of sulfur (ca. 15 mmol) was added to 250 mL of *n*-heptane in a three-necked flask equipped with a gas inlet, addition funnel, and reflux condenser. The suspension was vigorously stirred under a stream of carbon monoxide, which was maintained during the course of the reaction, and then warmed at ca. 35 °C. A solution of $Co_2(CO)_8$ (1.03 g, ca. 3 mmol) in 250 mL of *n*-heptane was added dropwise to the suspension, and the mixture was allowed to react until the dicobalt octacarbonyl disappeared (ca. 5 h). The solution contained complexes II, III, and IV in an approximate ratio of 1:1:2, respectively, together with part of the unreacted sulfur. The reaction mixture was filtered off, and pure IV could be obtained from the solution by two alternative ways.

Table I. Crystallographic Data for $Co_6(CO)_6S_8\cdot 3S_8$[a]

$C_6Co_6O_6S_{32}$
$a = 20.456$ (4) Å
$b = 12.385$ (4) Å
$c = 17.600$ (5) Å
$\beta = 90.94$ (2)°
$V = 4458.3$ Å^3
$Z = 4$
$R(F_o) = 0.048$

fw = 1547.82
space group: $C2/c$ (C_{2h}^6, No. 15)
$T = 20$ °C
$\lambda = 0.7107$ Å
$d_{calcd} = 2.31$ g cm^{-3}
$\mu = 35.34$ cm^{-1}
transm coeff = 0.678–0.998
$R_w(F_o) = 0.053$

[a] Here and in the subsequent table the esd's are given in parentheses.

Method a: Column Chromatography (Support, Silica Gel; Eluent, *n*-Heptane). Complex IV was eluted first as an olive green band, followed by III (red band) and finally by II (violet band). Black crystals of IV were obtained by concentrating the eluate to ca. 50 mL and cooling to −20 °C.

Method b: Fractional Crystallization. This method made use of the different solubilities, which are in the order II ≫ IV > III. The solution was concentrated to ca. 200 mL and stored at −20 °C. Most of the III present crystallized, together with some S_8. The filtered solution was concentrated again to 70–80 mL and allowed to stand overnight at −20

[†] Università di Torino.
[‡] Eidgenössische Technische Hochschule.
[§] Università di Sassari.

(1) Gervasio, G.; Rossetti, R.; Stanghellini, P. L.; Bor, G. *Inorg. Chim. Acta* **1984**, *83*, L9.
(2) E.g.: *Gmelins Handbuch der anorganischen Chemie*; Verlag Chemie: Weinheim, FRG, 1973; Band 6, Kobalt-Organisches Verbindungen.
(3) Markó, L.; Bor, G.; Almásy, G. *Chem. Ber.* **1961**, *94*, 847.
(4) Markó, L.; Bor, G.; Klumpp, E. *Chem. Ind.* (*London*) **1961**, 1491.
(5) Markó, L.; Bor, G.; Klumpp, E.; Markó, B.; Almásy, G. *Chem. Ber.* **1963**, *96*, 955.
(6) Khattab, S. A.; Markó, L. *Acta Chim. Acad. Sci. Hung.* **1964**, *40*, 471.
(7) Markó, L. *Gazz. Chim. Ital.* **1979**, *109*, 247.
(8) Wei, C. H.; Dahl, L. F. *Inorg. Chem.* **1967**, *6*, 1229. Strouse, C. E.; Dahl, L. F. *Discuss. Faraday Soc.* **1969**, *47*, 93.
(9) Stevenson, D. L.; Magnuson, V. R.; Dahl, L. F. *J. Am. Chem. Soc.* **1967**, *89*, 3727.
(10) Wei, C. H.; Dahl, L. F. *Cryst. Struct. Commun.* **1975**, *4*, 583.
(11) Klumpp, E.; Markó, L.; Bor, G. *Chem. Ber.* **1964**, *97*, 926.
(12) Klumpp, E.; Bor, G.; Markó, L. *Chem. Ber.* **1967**, *100*, 1451; *J. Organomet. Chem.* **1968**, *11*, 207.
(13) Bor, G.; Dietler, U. K.; Stanghellini, P. L.; Gervasio, G.; Rossetti, R.; Sbrignadello, G.; Battiston, G. A. *J. Organomet. Chem.* **1981**, *213*, 277.
(14) Gervasio, G.; Rossetti, R.; Stanghellini, P. L.; Bor, G. *Inorg. Chem.* **1982**, *21*, 3781.
(15) Bor, G.; Markó, B.; Markó, L. *Acta Chim. Acad. Sci. Hung.* **1961**, *27*, 395.

Table II. Fractional Atomic Coordinates and Temperature Factors ($Å^2 \times 10^4$) of the Asymmetric Unit for $Co_6(CO)_6S_8 \cdot 3S_8$

atom	x/a	y/b	z/c	U_{eq}
Co1	0.254 51 (4)	0.183 18 (6)	0.102 91 (4)	363 (2)
Co2	0.330 70 (3)	0.332 68 (6)	0.023 49 (4)	359 (2)
Co3	0.196 90 (3)	0.370 63 (6)	0.041 13 (4)	352 (2)
C11	0.258 95 (32)	0.120 11 (50)	0.191 14 (36)	512 (21)
O11	0.262 34 (29)	0.078 34 (45)	0.248 03 (27)	780 (20)
C21	0.400 68 (29)	0.408 57 (53)	0.043 53 (36)	506 (21)
O21	0.445 99 (24)	0.458 21 (44)	0.056 08 (35)	808 (21)
C31	0.156 41 (27)	0.479 82 (47)	0.082 39 (34)	439 (18)
O31	0.131 26 (23)	0.549 91 (38)	0.111 79 (29)	656 (17)
S1	0.275 24 (7)	0.355 51 (11)	0.129 99 (8)	400 (4)
S2	0.148 75 (7)	0.227 48 (11)	0.093 01 (8)	397 (4)
S3	0.232 06 (7)	0.040 70 (11)	0.030 11 (8)	403 (4)
S4	0.358 12 (7)	0.169 04 (12)	0.065 74 (8)	407 (4)
S5	0.360 86 (10)	0.159 32 (16)	0.729 99 (10)	653 (6)
S6	0.419 07 (12)	0.042 43 (17)	0.684 85 (12)	772 (8)
S7	0.498 35 (10)	0.116 98 (25)	0.639 22 (13)	925 (10)
S8	0.481 42 (10)	0.132 01 (21)	0.525 21 (12)	808 (8)
S9	0.447 69 (13)	0.283 51 (20)	0.505 33 (15)	934 (9)
S10	0.348 95 (13)	0.276 08 (21)	0.493 74 (12)	882 (9)
S11	0.308 92 (11)	0.323 90 (18)	0.594 36 (13)	782 (8)
S12	0.286 07 (9)	0.187 86 (18)	0.654 14 (13)	730 (7)
S13	0.026 29 (18)	0.275 99 (23)	0.702 11 (17)	1186 (13)
S14	0.103 83 (13)	0.180 61 (37)	0.722 56 (18)	1334 (16)
S15	0.087 21 (18)	0.033 96 (34)	0.674 17 (16)	1453 (17)
S16	0.051 71 (30)	−0.065 09 (31)	0.754 49 (23)	2169 (28)

°C. Crude crystals of IV were obtained with trace impurities of III; pure complex IV was finally recovered by subsequent recrystallization from *n*-heptane.

Procedure a is preferred when a small amount of material (100–200 mg) is handled; otherwise, procedure b is recommended.

Both procedures gave rise to similar yields, ca. 20% of complex IV based on $Co_2(CO)_8$).

Yellow crystals of free S_8 accompanied some of the crystallized products; these were mechanically eliminated by the help of a microscope. Different attempts to obtain crystals of $Co_6(\mu_3\text{-}S)_8(CO)_6$ free of intercluster S_8 rings were unsuccessful and resulted in the complete decomposition of the cluster compound.

Reagents and Instrumentation. $Co_2(CO)_8$ (Strem Chemical) was used as received; sulfur was purified by vacuum sublimation. The solvents were reagent grade and used without further purification. Merck silica gel G60 F-254 and Silica Woelm TSC were the supports for TLC and column chromatography, respectively.

IR spectra were recorded by a Bruker FT-IR spectrometer, Model IFS 113V. Raman spectra were taken with the Bruker FRA 106 FT-Raman module, attached to the IFS 66 FT-IR spectrometer (laser power 130 mw, resolution 8 cm^{-1}).

Crystal Data Collection. The reflections intensities were collected on a Nicolet R(3) automatic four-cycle diffractometer. The crystal data and some experimental conditions are listed in Table I; the full-length table collecting the experimental conditions appears in the supplementary material.

The crystal used for data collection was mounted without any special precaution owing to its good stability in air. The unit cell parameters were obtained with the use of 25 accurately centered reflections. No decrease of the check reflection was observed. The absorption correction was applied according to the method of ref 16; anomalous atomic scattering factors were applied according to ref 17; secondary extinction correction was not applied.

Resolution of the Structure. The Co atoms were located with the use of Patterson maps and by direct methods with the use of SHELX 76[18] programs. Subsequent difference Fourier maps revealed the S, C, and O atoms of the cluster and the S_8 molecules: one of these lies in a general position; the other one lies on a 2-fold axis.

In the expression of weight used ($w = 1/(\sigma(F)^2 + aF^2)$, a corresponds to a satisfying behavior of $\sum w/\Delta^2$ in various ranges of $(\sin\theta)/\lambda$ and $|F_o|$.

All the atoms were refined anisotropically; only the S_8 molecule on the 2-fold axis showed a slightly higher thermal motion. The root-mean displacements of atoms along the principal axes of their vibration ellipsoids are listed in Table II.

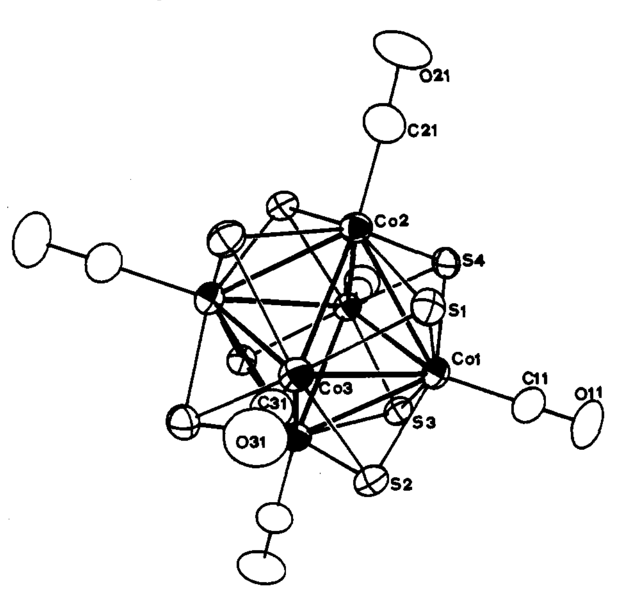

Figure 1. ORTEP drawing of the molecule with thermal ellipsoids of 36% probability and the atom-labeling scheme of the asymmetric portion of the molecule.

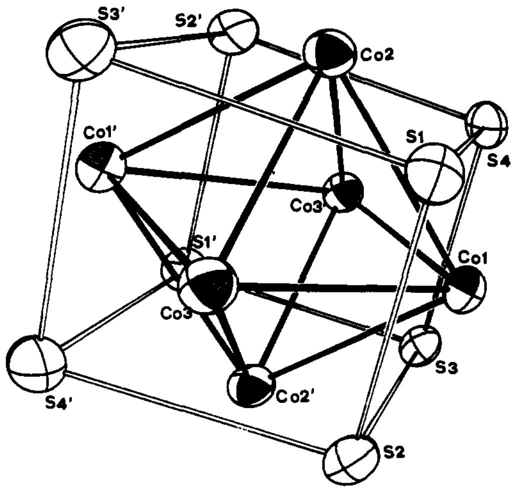

Figure 2. ORTEP drawing of the Co_6 octahedron compenetrated with the S_8 cube. The nonbonding S···S distances in the cube are as follows: S1···S2 = 3.094 (2) Å, S1···S3′ = 3.099 (2) Å, S1···S4 = 3.090 (2) Å, S2···S3 = 3.088 (2) Å, S2···S4′ = 3.076 (2) Å, and S3···S4 = 3.085 (2) Å. The label S′ corresponds to atoms related by the inversion center inside the molecule.

The final atomic fractional coordinates are listed in Table II; the bond distances and the bond angle values are reported in Table III. Lists of observed and calculated structure factors and of thermal anisotropic parameters are available as supplementary material.

Description of the Structure

Figure 1 shows the $Co_6(\mu_3\text{-}S)_8(CO)_6$ molecule with appropriate numbering of atoms. The Co_6S_8 core can be described as an octahedron of cobalt atoms, whose triangular faces are all bridged by an S atom, or, alternatively, as an assembly of an S_8 cube and a Co_6 octahedron having a common center, which is the crystallographic inversion center (Figure 2).

---

(16) North, A. C. T.; Phillips, D. C.; Mathews, F. S. *Acta Crystallogr., Sect. A: Cryst. Phys., Diffr., Theor. Gen. Crystallogr.* **1968**, *A24*, 351.

(17) Cromer, D. T.; Liberman, D. *J. Chem. Phys.* **1970**, *53*, 1891.

(18) Sheldrick, G. M. *SHELX 76, A System of Computer Programs*; Cambridge University: Cambridge, England, 1976.

(19) Albano, V. G.; Braga, D.; Martinengo, S. *J. Chem. Soc., Dalton Trans.* **1986**, 981.

(20) Hart, D. W.; Teller, R. G.; Wei, C. Y.; Bau, R.; Longoni, G.; Campanella, S.; Chini, P.; Koetzle, T. *J. Am. Chem. Soc.* **1981**, *103*, 1458.

(21) Albano, V. G.; Bellon, P. L.; Chini, P.; Scatturin, V. *J. Organomet. Chem.* **1969**, *16*, 461.

(22) Albano, V. G.; Chini, P.; Scatturin, V. *J. Organomet. Chem.* **1968**, *15*, 423.

(23) Albano, V. G.; Chini, P.; Ciani, G.; Sansoni, M.; Martinengo, S. *J. Chem. Soc., Dalton Trans.* **1980**, 163.

(24) Ciani, G.; Martinengo, S. *J. Organometal. Chem.* **1986**, *306*, C49.

Table III. Interatomic Distances (Å) and Selected Bond Angles (deg) for $Co_6(CO)_6S_8{\cdot}3S_8$

$Co_6(CO)_6S_8$ Cluster[a]			
Co1–Co2	2.8076 (12)	Co2–S4	2.2274 (18)
Co1–Co3	2.8140 (12)	Co2–S2′	2.2282 (17)
Co1–Co2′	2.8105 (12)	Co2–S3′	2.2266 (16)
Co1–Co3′	2.8182 (12)	Co2–C21	1.7437 (62)
Co1–S1	2.2261 (17)	Co3–S1	2.2287 (16)
Co1–S2	2.2359 (17)	Co3–S2	2.2308 (16)
Co1–S3	2.2243 (16)	Co3–S3′	2.2248 (16)
Co1–S4	2.2352 (17)	Co3–S4′	2.2309 (17)
Co1–C11	1.7394 (64)	Co3–C31	1.7498 (59)
Co2–Co3	2.7994 (10)	C11–O11	1.1282 (80)
Co2–Co3′	2.8163 (13)	C21–O21	1.1310 (80)
Co2–S1	2.2250 (17)	C31–O31	1.1379 (76)
S4–Co1–C11	100.97 (24)	S2′–Co2–S3′	87.81 (8)
S3–Co1–C11	99.52 (21)	S4–Co2–C21	102.80 (22)
S3–Co1–S4	87.54 (8)	S1–Co2–C21	100.91 (23)
S2–Co1–C11	102.48 (24)	S1–Co2–S3′	88.23 (9)
S2–Co1–S4	156.53 (10)	S1–Co2–S4	87.91 (8)
S2–Co1–S3	87.67 (9)	Co3–Co2–C21	133.47 (22)
S1–Co1–C11	103.44 (22)	Co3–Co2–S4	110.92 (9)
S1–Co1–S4	87.68 (8)	Co3–Co2–S1	51.12 (7)
S1–Co1–S3	157.04 (9)	Co1–Co3–Co2	60.02 (5)
S1–Co1–S2	87.83 (8)	Co2–Co3–C31	130.25 (21)
Co3–Co1–C11	136.96 (22)	Co2–Co3–S2	110.55 (7)
Co3–Co1–S4	110.16 (7)	Co2–Co3–S1	51.00 (7)
Co3–Co1–S3	110.53 (8)	Co2–Co3–Co2′	89.71 (6)
Co3–Co1–S2	50.87 (6)	Co2–Co3–Co1′	60.04 (6)
Co3–Co1–S1	50.87 (6)	Co1–Co3–C31	132.48 (21)
Co3–Co1–Co3′	89.95 (5)	Co1–Co3–S2	51.03 (6)
Co3–Co1–Co2′	60.09 (4)	Co1–Co3–S1	50.78 (5)
Co2–Co1–C11	136.00 (23)	Co1–Co3–Co1′	90.05 (5)
Co2–Co1–S4	50.89 (6)	S4′–Co3–C31	106.53 (21)
Co2–Co1–S3	110.33 (8)	S3′–Co3–C31	99.81 (20)
Co2–Co1–S2	110.10 (6)	S3′–Co3–S4′	87.63 (9)
Co2–Co1–S1	50.87 (6)	S2–Co3–C31	103.25 (21)
Co2–Co1–Co3′	60.08 (4)	S1–Co3–C31	96.52 (22)
Co2–Co1–Co2′	89.66 (6)	S1–Co3–S2	87.89 (9)
Co2–Co1–Co3	59.73 (5)	Co2–S1–Co3	77.89 (9)
Co1–Co2–C21	135.67 (23)	Co1–S1–Co3	78.35 (7)
Co1–Co2–S4	51.14 (6)	Co1–S1–Co2	78.21 (7)
Co1–Co2–S1	50.91 (6)	Co1–C11–O11	179.18 (62)
Co1–Co2–Co3	60.25 (5)	Co2–C21–O21	179.52 (62)
S3′–Co2–C21	99.89 (23)	Co3–C31–O31	177.37 (57)
S2′–Co2–C21	101.52 (22)		
S_8 Molecules[b]			
S5–S6	2.0435 (30)	S11–S12	2.0446 (32)
S5–S12	2.0447 (28)	S13–S13′	2.0145 (46)
S6–S7	2.0421 (33)	S13–S14	2.0055 (49)
S7–S8	2.0393 (32)	S14–S15	2.0323 (59)
S8–S9	2.0276 (36)	S15–S16	2.0161 (56)
S9–S10	2.0289 (38)	S16–S16′	2.1189 (87)
S10–S11	2.0507 (33)		
S6–S5–S12	107.65 (14)	S10–S11–S12	107.72 (15)
S5–S6–S7	107.71 (15)	S5–S12–S11	107.67 (15)
S6–S7–S8	107.77 (16)	S13–S14–S15	108.95 (21)
S7–S8–S9	107.82 (16)	S13′–S13–S14	106.34 (21)
S8–S9–S10	108.11 (16)	S14–S15–S16	108.04 (23)
S9–S10–S11	108.12 (18)	S15–S16–S16′	108.56 (25)

[a] Atoms marked with a prime in this section are generated by the inversion center at $^1/_4$, $^1/_4$, 0. [b] Atoms marked with prime in this section are generated by the 2-fold axis.

Table IV. Co–Co Distances (Å) in Octahedral Co_6 Clusters

complex	d(Co–Co), Å	ref
$[Co_6C(CO)_{13}]^{2-}$[a]	2.465 (1)–2.926 (1)	19
$[HCo_6(CO)_{15}]^{-}$[a]	2.490 (2)–2.661 (2)	20
$[Co_6(CO)_{14}]^{4-}$[a]	2.466 (2)–2.534 (2)	21
$[Co_6(CO)_{15}]^{2-}$[a]	2.454 (4)–2.532 (4)	22
$[Co_6C(CO)_{14}]^{-}$[b]	2.519 (4)–2.916 (4)	23
$[Co_6N(CO)_{13}]^{-}$[a]	2.487 (5)–2.788 (5)	24
$Co_6S_8(PEt_3)_6$[c]	2.814 (2)–2.818 (2)	25
$Co_6S_8(PPh_3)_6$[c]	2.990 (2)–3.020 (2)	26, 27
$Co_6S_8(CO)_6$[c]	2.799 (1)–2.818 (1)	this work
$[Co_6S_8(PEt_3)_6]^{+}$[d]	2.771 (4)–2.808 (3)	28
$[Co_6S_8(PPh_3)_6]^{+}$[d]	2.798 (2)–2.828 (2)	29
$[Co_6S_8(PPh_3)_6]^{+}$[d]	2.860 (5)–2.930 (5)	27

[a] 86 valence electrons. [b] 87 valence electrons. [c] 98 valence electrons. [d] 97 valence electrons.

Table V. Symmetry Species of the Vibrational Modes of the $Co_6S_8(CO)_6$ Octahedral Cluster

	A_{1g}	E_g	T_{1g}	T_{2g}	A_{1u}	E_u	T_{1u}	T_{2u}
activity	R	R		R			IR	
Co–Co str	1	1		1			1	1
Co–S str	1	1	1	2	1	1	2	1
C–O str	1	1					1	
Co–CO str	1	1					1	
Co–C–O def			1	1			1	1
Co–Co–C def			1	1			1	1
tot.	4	4	3	5	1	1	7	4

The octahedral vertices project from the center of the cubic faces by about 0.44 Å and bear a terminal CO group.

The Co–Co distances span quite a wide range, indicating a significant distortion (differences of 19σ) of the metal core from the idealized octahedral symmetry. The Co_6 polyhedron is usually somewhat distorted, as illustrated in Table IV. The average Co–Co distance are already grouped around to two characteristic values, ca. 2.52 Å for the 86 valence electron clusters and ca. 2.80 Å for the 97–98 valence electron clusters. The difference is significant and may be explained in terms of the analysis of the metal–metal bonding (see later).

The sulfur atoms formally describe a cube (Figure 2); the S···S distances are nonbonding but significantly less than sum of the van der Waals radii, as evidenced also in the analogous $Co_6Se_8(PPh_3)_6$ complex.[27] The cube is rather distorted (difference of 8σ among the S···S distances), and at least one S_4 plane is strongly puckered.[30]

The Co–S bonding distances are very close to those of the other Co_6S_8 systems and are significantly longer than the Co–S distances in $Co_3(\mu_3\text{-}S)$ triangular fragments of cobalt carbonyl clusters.[31] The longest Co–S distances belong to the compounds that show at same time the longest Co–Co distances. Complexes like $Co_4Cp_4S_4$,[37] $[Co_4Cp_4S_4]^+$,[37] $Co_4Cp_4S_6$,[38] and $[Co_3(\mu_3\text{-}S)(SCH_2)_2C_6H_4)_3]^{2-}$[39] where the Co–S distances are long and the Co–Co distances are quite nonbonding (≥3.2 Å in the Co_4 systems) or long (2.715–2.825 Å in the Co_3 complex) confirm the trend. Even the values of the Co–S distances are spread out in a limited

---

(25) Cecconi, F.; Ghilardi, C. A.; Midollini, S.; Orlandini, A. *Inorg. Chim. Acta* **1983**, *76*, L183.

(26) Fenske, D.; Ohmer, J.; Hachgenei, J. *Angew. Chem., Int. Ed. Engl.* **1985**, *24*, **1985**, 993.

(27) Fenske, D.; Ohmer, J.; Merzweiler, K. *Z. Naturforsch., B* **1987**, *42*, 803.

(28) Cecconi, F.; Ghilardi, C. A.; Midollini, S. *Inorg. Chim. Acta* **1982**, *64*, L47.

(29) Fenske, D.; Hachgenei, J.; Ohmer, J. *Angew. Chem. Int. Ed. Engl.* **1985**, *24*, 706.

(30) The equation of the S1S2S3S4 average plane in fractional coordinates is $0.641x - 5.16y + 15.98z = 0.41$, which gives rise to $\chi^2 = 21.0$ and to the values of the distance from the plane of 0.006 (2) Å for S1 and S3 and of −0.006 (2) for S2 and S4. The other planes are more regular. S1S2′S3′S4 plane: equation $16.99x + 6.40y + 3.41z = 7.39$; distances from plane 0.003 (2) Å for S1 and S2′, −0.003 (2) Å for S3′ and S4; $\chi^2 = 4.44$. S1S2S3′S4′ plane: equation $11.31x + 9.29y + 6.54z = 1.04$; distances from plane 0.000 (2) Å for all the atoms; $\chi^2 = 0.05$.

(31) E.g.: $Co_3(CO)_9S$ (2.139 (4) Å),[32] $[Co_3(CO)_7S]_2S_2$ (2.144 (6) Å),[33] $Co_3(C_5H_5)_3S_2$ (2.157 (3) Å),[34] SCo_3 residue in $SCo_6(CO)_{11}S(C_2H_5)_4$ (2.163 (6) Å),[35] $Co_6(CO)_{16}C_2S_3$ (2.153 (2) Å),[14] $Co_6(CO)_{15}CS_3$ (2.156 (1) Å),[14] $Co_6(CO)_{16}C_2S_4$ (2.17 (1) Å).[36]

(32) Wei, C. H.; Dahl, L. F. *Inorg. Chem.* **1967**, *6*, 1229.

(33) Stevenson, D. L.; Magnuson, V. R.; Dahl, L. F. *J. Am. Chem. Soc.* **1967**, *89*, 3727.

(34) Frish, P. D.; Dahl, L. F. *J. Am. Chem. Soc.* **1972**, *94*, 5082.

(35) Wei, C. H.; Dahl, L. F. *J. Am. Chem. Soc.* **1968**, *90*, 3977.

(36) Wei, C. H. *Inorg. Chem.* **1984**, *23*, 2973.

(37) Simon, G. L.; Dahl, L. F. *J. Am. Chem. Soc.* **1973**, *95*, 2164.

(38) Uchtmann, V. A.; Dahl, L. F. *J. Am. Chem. Soc.* **1969**, *91*, 3756.

(39) Henkel, G.; Tremel, W.; Krebs, B. *Angew. Chem., Int. Ed. Engl.* **1983**, *22*, 318.

Table VI. Frequency Values (cm^{-1}) and Assignments of the Vibrational Absorptions of the $Co_6S_8(CO)_6{\cdot}3S_8$ Complex

$Co_6S_8(CO)_6{\cdot}3S_8$			free S_8[a]		
IR[b]	Raman[c]	assignt	IR[b]	Raman	assignt
	2074 v, br	$\nu(CO)$ (A_{1g})			
2058 vs[d]		$\nu(CO)$ (T_{1u})			
2053 vs					
2046 vs		$\nu(CO)$ (A_u (T_{1u}-der.))			
	2048 w, br	$\nu(CO)$ (E_g)			
2035 vs		$\nu(CO)$ (A_u (T_{1u}-der.))			
2006 w					
2002 w		^{13}CO			
1992 w					
517 s		$\delta(Co\text{–}C\text{–}O)$ (T_{1u})			
472 m		S_8	472 m		E_1
	470 s	S_8		470 s	A_1
	434 m	S_8		434 m	E_3
	395 vw	$\nu(Co\text{–}CO)$ (A_{1g})			
375 m		$\nu(Co\text{–}CO)$ (T_{1u})			
	360 m	$\nu(Co\text{–}CO)$ (E_g)			
	315 vw	$\nu(Co\text{–}S)$ (A_{1g})			
315 w		$\nu(Co\text{–}S)$ (T_{1u})			
	280 m	$\nu(Co\text{–}S)$ (T_{2g})			
240 w		S_8	243 s		B_2
	240 m	S_8		243 w	E_3
	217 s	S_8		216 s	A_1
	195 w	S_8		191 w	E_1
188 w		$\delta(Co\text{–}S\text{–}Co) + \nu(Co\text{–}Co)$ (T_{1u})			
	151 s	S_8		152 s	E_2
72 w		$\delta(Co\text{–}Co) + \delta(Co\text{–}Co\text{–}C)$ (T_{1u})			

[a] Data from Ref 41. [b] Spectrum run on KBr disk (2100–300 cm^{-1}) and on polyethylene disk (300–50 cm^{-1}). [c] Spectrum run on microcrystalline powder. [d] Spectrum run on *n*-heptane solution.

range (2.224–2.236 Å): owing to the symmetry of the molecule, all these distortions apparently have no physical meaning, but are probably due to the packing effect of the molecule in the lattice.

The data concerning the S_8 rings have quite normal values (2.04 Å, 107.9° on the average), taking into account also the high thermal motion of one of them. The distances between the S_8 rings and the cluster molecules are large enough (contacts greater than the sum of the van der Waals radii) to exclude any chemical interaction.

Vibrational Analysis

Symmetry Properties. $Co_6S_8(CO)_6$ has 72 normal modes of vibration that are distributed among the symmetry species of the idealized symmetry group (O_h) in Table V.

To set up valence-type internal coordinates, the Co_6S_8 core must be considered first. As the number of its normal modes is exactly equal to the number of the edges (36), the vibrations of the core are fully described by means of the bond stretches exclusively.[40] In reality, the vibrations of the core are mixtures of bond stretching and angle deformation displacements. In particular, the Co–S modes can alternatively be described as motion of the S atoms perpendicular to or parallel to the Co_3 triangle. The perpendicular motions are of $A_{1g} + T_{2g} + A_{2u} + T_{1u}$ type and have primarly a Co–S stretching character; the others, belonging to the remaining Co–S species, are predominantly of Co–S–Co bending character.

The six coordinated CO groups give rise to 36 normal modes including the nongenuine (i.e. transational and vibrational) ones, which may be divided into C–O stretchings, Co–CO stretchings, Co–C–O deformations, and Co–Co–C deformations. The symmetry species are illustrated in Table V.

We wish to point out a small but singular detail of the "character" of the normal vibration of the cluster. The 72 normal modes of the entire $Co_6S_8(CO)_6$ have been divided into 36 modes, belonging to the Co_6S_8 core, and 36 modes due to the motion of the CO groups. However, if we consider the core as one rigid block "M", the unit "M"$(CO)_6$ has only 33 normal modes. What is the explanation for the difference of 3? The contradiction is only apparent and can be easily ruled out if we consider that the "real" core, i.e. the Co_6S_8 octahedron, is not pointlike. The missing three modes must have the character connected to the "nonpointlike" nature of the core. This must be a triply degenerate "pseudorotational" (or librational) sort of vibration of the rigid core relative to the "shell" of the six carbonyl ligands: clearly a T_{1g} mode, since the rotations themselves belong to this species.

All the T_{1g} modes for the $M(CO)_6$ and $(Co_6S_8)(CO)_6$ systems are depicted in Figure 3, from which is clear that the nonpointlike nature of the Co_6S_8 core generates a new genuine vibrational mode, approximately described as Co–Co–C deformation. This sort of splitting between these skeletal modes is largely formal, as we expect that these types of motions are strongly coupled.

Assignment of the Absorptions (Table VI). (a) CO Stretching Zone. The expected spectral pattern is very simple, one infrared and two Raman bands, belonging to the T_{1u} and A_{1g} and E_g modes, respectively. The T_{1u} mode is easily assigned to the unique IR band in the solution spectrum at 2058 cm^{-1}; unfortunately, the low solubility of the complex did not allow us to get a suitable solution Raman spectrum.

The solid-state Raman spectrum shows two weak broad absorptions at 2074 and 2048 cm^{-1}, which can reasonably be interpreted on a molecular basis, taking into account that the Raman data (nondipolar modes) are less subject to solid-state interactions: the assignment is A_{1g} and E_g, respectively. The infrared spectrum shows three strong absorptions at ca. 2053, 2046, and 2035 cm^{-1}: they are presumably due to a site-group splitting of the T_{1u} mode, which gives rise to three A_u modes under the C_i site symmetry. This is supported by the three ^{13}CO peaks around 2000 cm^{-1}. The large unit cell and the presence of the S_8 groups between the cluster molecules render the intermolecular CO couplings unlikely, so presumably factor group effects are excluded.

(b) Medium–Low Frequency Zone. The intermolecular couplings are usually not important with the low-energy vibrational modes, so the spectral data can be reasonably interpreted on molecular basis.

The solid-state Raman spectrum is dominated by three strong bands at 470, 217, and 151 cm^{-1}: they correspond very closely to the three fundamental modes of the S_8 molecule, which give rise to most intense absorptions in the relevant Raman spectrum.[41]

---

(40) Brunvoll, J.; Cyvin, S. J. *Skr.—K. Nor. Vidensk. Selsk.* **1967**, *3*, 3.

(41) Scott, D. W.; McCullough, J. P.; Kruse, F. H. *J. Mol. Spectrosc.* **1964**, *13*, 313.

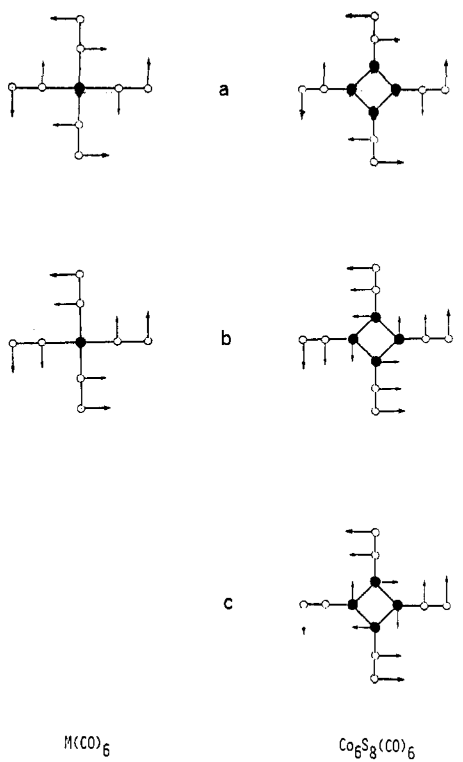

Figure 3. Schematic description of (a) M-C-O deformation and (b) rotational and (c) "pseudorotational" or M-M-C deformation T_{1g} modes.

The coincidence between the two spectra demonstrates that the vibrations of the S_8 molecules cocrystallized with the cluster are practically unchanged with respect to those of the free S_8. This guideline allows one to reasonably assign in terms of the local point symmetry of S_8 (D_{4d}) the Raman medium-weak bands at 434, 240, and ca. 195 cm^{-1} to the Raman-active E_3 and E_1 modes and the infrared absorptions at 472 and 240 cm^{-1} to the IR-active E_1 and B_2 modes of the S_8 molecule in the lattice. It is noteworthy that, in free S_8, the A_1 (Raman) and E_1 (infrared) modes have accidentally coincident frequency values (ca. 472 cm^{-1}), like the E_3 (Raman) and B_2 (infrared) modes at 243 cm^{-1}. The same coincidences are evident in the spectra of the mixed S_8–cluster crystal.

The "true" vibrational modes of the cluster are clearly recognized in the infrared spectrum. Six infrared-active T_{1u} modes are expected in this region (see Table V) and five bands are clearly recognized in the spectra (Figure 5 and Table VI). The highest frequency bands are straightforwardly assigned to the Co–C–O deformation (at 517 cm^{-1}) and to the Co–CO stretching (at 375 cm^{-1}). Moreover, the band at 315 cm^{-1} presumably belongs to the Co–S mode with prevailing stretching character. The remaining absorptions at 188 and 72 cm^{-1} are probably a mixture of Co–S–Co deformation, Co–Co stretching and Co–Co–C deformation. The missing T_{1u} mode has probably too low intensity and/or frequency to be detected.

The assignment of the cluster Raman-active modes is largely tentative, because of the weakness of the absorption and the poor resolution of the spectrum. We suggest that the two weak bands at ca. 395 and 360 cm^{-1} are ν(Co–CO) modes of A_{1g} and E_g symmetry, respectively, whereas the other two absorptions at ca. 315 and 280 cm^{-1} could be the remaining ν(Co–S) modes of A_{1g} and T_{2g} symmetry.

Description of the Bonding

In the MO schemes of the most common M_6 octahedral metal clusters with 86 valence electrons,[42] the order of the MO levels

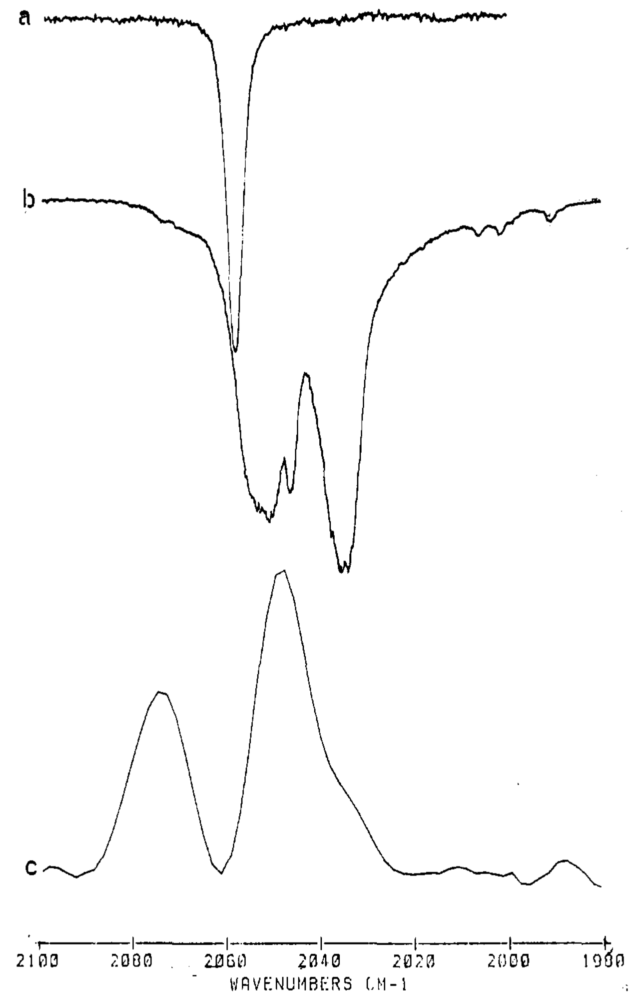

Figure 4. $Co_6S_8(CO)_6$ spectra in the CO stretching region: (a) IR spectrum of the *n*-heptane solution; (b) IR spectrum for a KBr disk at ca. 100 K; (c) Raman spectrum of the crystals.

agrees on the gross features, although little differences appear because of the different procedures of calculation. For example, the MO's of the naked M_6 core are separated in the so-called d band, s band, and p band, the last one showing a large gap between 11 high energy levels and the other levels with s or p origin. This accounts for 43 metal orbitals only, which are able to interact with the ligand orbitals, giving rise to 43 strongly or weakly bonding molecular orbitals with a large HOMO–LUMO gap: so the "magic number", 86 electrons, is largely justified.

This model does not seem very suited for $Co_6S_8(CO)_6$, which should accommodate 12 out of its 98 valence electrons (54 from the cobalt atoms, 32 from the sulfur atoms, and 12 from the CO groups) in strongly antibonding orbitals: any realistic model ought to have 49 bonding or weakly antibonding molecular orbitals. Bottomley and Grein[43] proposed a model for $Cp_nM_n(\mu_3\text{-}A)_m$ (A = O, S) clusters, in which a group of 12 orbitals at high energy, essentially metal in character, can accommodate the "excess" electrons, i.e., the electrons exceeding those involved in the metal–ligand bonds. The energy order of the 12 levels is determined by a combination of the M–M, the M–Cp, and the M–A bonding and, for an octahedral cluster ($n = 6$, $m = 8$), shows a large gap between five high levels (e_g and t_{1u}) and seven low levels (a_{2g}, t_{2g}, e_g, and a_{1g}). The present cluster has 14 "excess" electrons,[44] which can exactly fill the low-energy set of the "excess" orbitals. As the relative order of the energy levels was reported

---

(42) Mingos, D. M. P. *J. Chem. Soc., Dalton Trans.* **1974**, 133; **1976**, 1163. Lauher, J. W. *J. Am. Chem. Soc.* **1978**, *100*, 5305. Woolley, R. G. *Inorg. Chem.* **1985**, *24*, 3519. Johnston, L. R.; Mingos, D. M. P. *Inorg. Chem.* **1986**, *25*, 1661.

(43) Bottomley, F.; Grein, F. *Inorg. Chem.* **1982**, *21*, 4170.

(44) According to the B&G model, the "excess" electrons are equal to 98 − $2x(8n_S + 6n_{CO})$, where $n_S = 3$ is the number of bonds formed by each S atom and $n_{CO} = 3$ is the number of bonds ($1\sigma + 2\pi$) formed by each CO group.

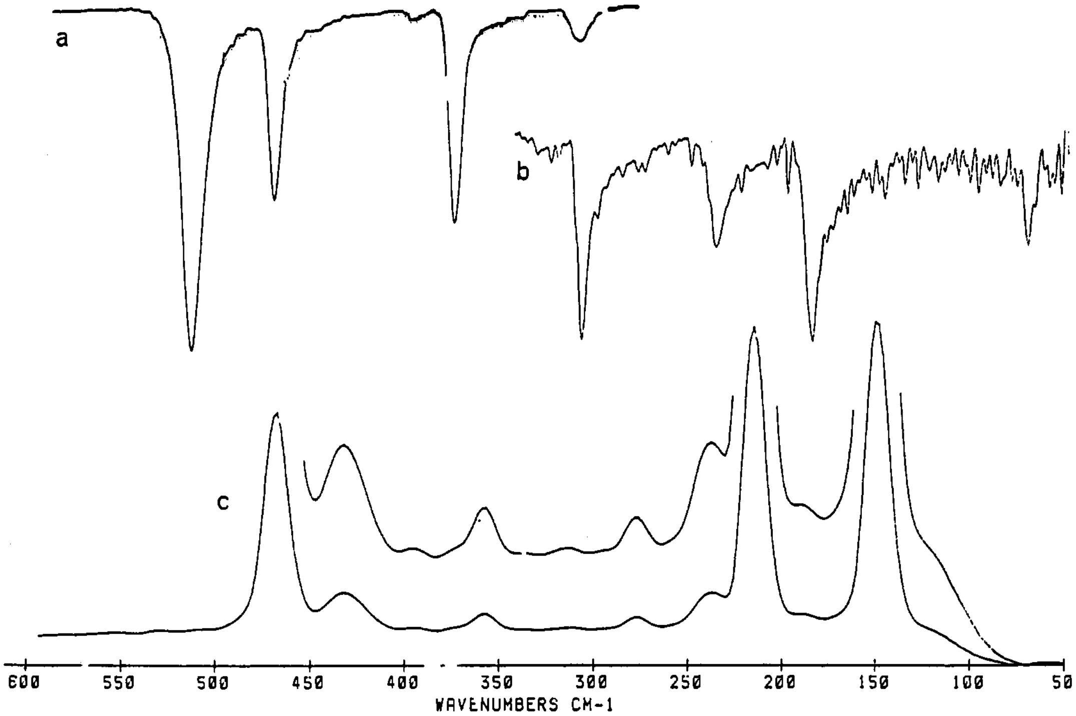

Figure 5. $Co_6S_8(CO)_6$ spectra in the 600–50-cm^{-1} region: (a) IR spectrum for a KBr disk; (b) IR spectrum for a polyethylene disk; (c) Raman spectrum of the crystals.

to be not significantly dependent on M and A, this model may satisfactorily explain the electronic structure of the cluster.

Similar results have been reached by the MO calculation made by Burdett[45] on the Mo_6S_8 molecular fragment of the Chevrel phases. The orbital diagram clearly shows that five MO's, molybdenum 5p combinations with e_g and t_{1u} symmetry, are greatly separated (by more than 15 eV) from the other orbitals. If similar behavior is expected, at least qualitatively, for the Co_6S_8 system, only 5 molecular orbitals among the total of 54 are wholly inaccessible to the bonding: so it is possible to accommodate 98 electrons at most. The complete filling of the 49 orbitals may account for the chemical stability and the diamagnetism of the complex. Similar conclusions were reached for another 98-electron cluster $Cp_6Ni_2Zn_4$.[46]

The principal difference between the 86- and the 98-electron octahedral M_6 clusters consists of six additional filled orbitals for the latter. As they are p_x and p_y combinations of t_{1g} and t_{1u} symmetry, they can be suitable to match a good interaction with similar combinations of orbitals of the CO groups bonded to the Co atoms. The net effect is a charge transfer from the metal to the carbonyl (π-back-donation), presumably required by the high electron content of the inner core.

Furthermore, in the Hoffmann model of the Chevrel phases,[47] the packing of the Mo_6S_8 units in the extended solid is due to the bonding between the Mo atoms and the S atoms of the neighboring clusters along the local C_4 axis. The symmetry of these "external" S atoms and, presumably, their bonding effect are close to those of the CO groups coordinated to the Co_6S_8 cluster. Hoffmann described the intercluster Mo–S bonds as an interaction between chalcogen donor orbitals and cluster molecular orbitals, which have mainly d origin and metal–metal character. The main effect of this perturbation on the Mo_6S_8 cluster is the strong pushing up of some M–M levels of appropriate symmetry (a_{1g}, t_{1u}, and e_g). They are quite empty in the Mo_6S_8 system, but completely filled in the Co_6S_8 complex, where the consequence should be a large weakening of the metal–metal interaction: the very long value of the Co–Co distance is significant.

Acknowledgment. Financial support from the Ministero della Università e della Ricerca Scientifica e Tecnologica (Italy) is gratefully acknowledged. We thank Dr. A. Simon (Bruker GmbH, Karlsruhe, FRG) for running the Raman spectra.

Registry No. II, 15927-92-1; III, 57034-21-6; IV, 129787-39-9; $Co_2(CO)_8$, 10210-68-1.

Supplementary Material Available: PLUTO drawing of the cell content, projected down the *b* axis (Figure S1), and a full listing of crystal and experimental data (Table SI), principal axes of the thermal ellipsoids (Table SII), and anisotropic thermal parameters (Table SIII) (6 pages); a listing of observed and calculated structure factors (Table SIV) (19 pages). Ordering information is given on any current masthead page.

---

(45) Burdett, J. K.; Lin, J. H. *Inorg. Chem.* **1982**, *21*, 5.

(46) Budzelaar, P. H. M.; Boersma, J.; van der Kerk, G. J. M.; Spek, A. L.; Duisenberg, A. J. M. *Organometallics* **1985**, *4*, 680.

(47) Hughbanks, T.; Hoffmann, R. *J. Am. Chem. Soc.* **1983**, *105*, 1150.